

Filtering and LES of flow over irregular rough boundary

By A. Nakayama †, K. Hori † AND R. L. Street

Formal explicit filtering defined by the convolution integral over a flow region has been applied to derive fundamental equations of Large Eddy Simulation (LES) for turbulent flows over complex boundaries with small-scale roughness which is not resolved in full. It allows smoothing of the boundary at the same level of filtering as for the flow. It indicates that extra stress-like terms appear in the equations due to the smoothing. DNS data for a flow over a doubly wavy boundary are analyzed to examine the distributions of these terms and other quantities that need modeling. It is found that these stress terms are due to the pressure drag acting on smoothed-out roughness. Preliminary LES calculations have also been made to examine a model for these terms. It is suggested that the modeling of the boundary resistance terms must be done with appropriate modeling of the boundary conditions. A dynamic procedure to determine model constants is proposed.

1. Introduction

Numerical calculation of large scale flows appearing in natural environments almost always involves simplification of the boundary geometry. It is not only impossible but also meaningless to represent all the details of the terrain with trees and vegetation, not to mention smaller objects, in simulating an atmospheric wind field. Flows in rivers and oceans have an additional complex boundary on the free surface. The overall effects of small and random irregularities may be accounted for as roughness but larger undulations would have to be considered a part of the boundary shape. In fact the roughness and the boundary shape cannot be discriminated so easily. The numerical resolution of the flow field determines what should be considered roughness and what should be considered the boundary shape. If the small scale irregularities are smoothed out or ignored, the motion associated with the details is lost. In the context of large eddy simulation (LES), this will give rise to additional subgrid-scale stresses. It was suggested that small details of irregularities of bed materials like stones of various sizes and shapes in natural rivers are better treated by spatial averaging (Nikora *et al.* 2001), which also leads to an additional stress referred to as dispersion effects. In simulation of atmospheric boundary layers, the extra resistance due to the canopy is added in the flow (e.g. Brown *et al.* 2001; Chow & Street 2002).

In the previous report, we have conducted a Direct Numerical Simulation of a model flow over a doubly wavy surface. The small-scale waviness was intended to simulate roughness and the large-scale waviness the boundary shape. Here we consider modeling of such a flow over a complex boundary with superimposed roughness. First we derive the basic LES equations that result from filtering the instantaneous Navier-Stokes equations over the finite and irregular flow domain. Filtering in a finite domain introduces extra terms or commutation error terms. Modeling of the resulting equations is attempted

† Kobe University

making use of the DNS results. The flow field considered in the present work is assumed to be simply connected so that there are no pores or isolated objects in flow.

2. Filtering in complex finite flow domain

In order to explicitly filter the flow over finite boundary, we use the filtering operation defined by

$$\overline{f(\mathbf{x})} = \iiint_D G(\mathbf{x}, \boldsymbol{\xi}) f(\boldsymbol{\xi}) d\boldsymbol{\xi}, \quad (2.1)$$

where D is the actual flow domain and the filter function $G(\mathbf{x}, \boldsymbol{\xi})$ is related to a symmetric weight function $w(\mathbf{x} - \boldsymbol{\xi})$ by the normalization relation

$$G(\mathbf{x}, \boldsymbol{\xi}) = \frac{w((\mathbf{x} - \boldsymbol{\xi})/\Delta)}{W(\mathbf{x})}, \quad (2.2)$$

where Δ is the filter size and $W(\mathbf{x})$ is the total weight of w in the flow region,

$$W(\mathbf{x}) = \iiint_D w\left(\frac{\mathbf{x} - \boldsymbol{\xi}}{\Delta}\right) d\boldsymbol{\xi}. \quad (2.3)$$

The filter width Δ may be taken to depend on position, but here we consider the case when it is constant. If this filtering is applied to the divergence of a vector $\mathbf{F}(\mathbf{x})$, and the volume integral is evaluated by the divergence theorem, we have

$$\begin{aligned} \overline{\nabla \cdot \mathbf{F}(\mathbf{x})} &= \iiint_D G(\mathbf{x}, \boldsymbol{\xi}) \nabla_{\boldsymbol{\xi}} \cdot \mathbf{F}(\boldsymbol{\xi}) d\boldsymbol{\xi} \\ &= \iint_S G(\mathbf{x}, \boldsymbol{\xi}) \mathbf{F}(\boldsymbol{\xi}) \cdot \mathbf{n} dS_{\boldsymbol{\xi}} - \iiint_D \nabla_{\boldsymbol{\xi}} G(\mathbf{x}, \boldsymbol{\xi}) \cdot \mathbf{F}(\boldsymbol{\xi}) dV_{\boldsymbol{\xi}} \\ &= \iint_S G(\mathbf{x}, \boldsymbol{\xi}) F_n(\boldsymbol{\xi}) dS_{\boldsymbol{\xi}} - \iiint_D \frac{-\nabla_{\mathbf{x}}(w(\mathbf{x} - \boldsymbol{\xi})/\Delta)}{W(\mathbf{x})} \cdot \mathbf{F}(\boldsymbol{\xi}) dV_{\boldsymbol{\xi}} \\ &= \iint_S G(\mathbf{x}, \boldsymbol{\xi}) F_n(\boldsymbol{\xi}) dS_{\boldsymbol{\xi}} - \iiint_D \left[-\nabla_{\mathbf{x}} G(\mathbf{x}, \boldsymbol{\xi}) - G(\mathbf{x}, \boldsymbol{\xi}) \frac{\nabla_{\mathbf{x}} W(\mathbf{x})}{W(\mathbf{x})} \right] \cdot \mathbf{F}(\boldsymbol{\xi}) dV_{\boldsymbol{\xi}} \\ &= \overline{F_n}^S(\mathbf{x}) + \nabla \cdot \overline{\mathbf{F}(\mathbf{x})} + \frac{\nabla W}{W} \cdot \overline{\mathbf{F}(\mathbf{x})} \end{aligned} \quad (2.4)$$

where \mathbf{n} is the unit vector outward normal to the boundary S of flow domain D and subscript n is used to indicate the component of a vector in the direction of \mathbf{n} . The first term in the last line of this equation is the flux through the boundary filtered over the boundary, the second term is the divergence of the filtered \mathbf{F} and the last term is a quantity arising from the spatial variation of the total weight $W(\mathbf{x})$. An additional term would appear if Δ was a function of \mathbf{x} , corresponding to the commutation error due to varying filter size. If we take the filtered or "smoothed" boundary to be the surface given by $W(\mathbf{x}) = W_0 = \text{Const.}$ (Figure 1), the last term in Eq.(2.4) can be rewritten as follows

$$\frac{\nabla W}{W} \cdot \overline{\mathbf{F}} = \frac{\nabla W}{|\nabla W|} \frac{|\nabla W|}{W} \cdot \overline{\mathbf{F}} = -\chi \overline{\mathbf{n}} \cdot \overline{\mathbf{F}} = -\chi \overline{F_n} \quad (2.5)$$

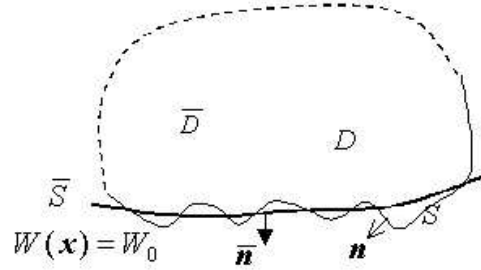


FIGURE 1. Filtering in complex flow domain.

where $\bar{\mathbf{n}} = -\nabla W/|\nabla W|$ is the outward unit normal vector on the smoothed boundary, $\chi = |\nabla W|/W$ is the relative change of the total weight and subscript \bar{n} indicates the component of a vector in the direction of $\bar{\mathbf{n}}$. χ is nonzero only in the layer next to the boundary with thickness roughly equal to the sum of the height of the smoothed boundary and the filter size. The last expression means that it is proportional to the filtered flux through the smoothed boundary.

Using this, Eq.(2.4) can be written as

$$\overline{\nabla \cdot \mathbf{F}(\mathbf{x})} = \nabla \cdot \overline{\mathbf{F}(\mathbf{x})} + \overline{F_n^S}(\mathbf{x}) - \chi \overline{F_{\bar{n}}}. \quad (2.6)$$

This means that the filter of a divergence is the divergence of the filter plus the difference between the flux through the original boundary and the filtered flux through the smoothed boundary. The corresponding formula for the gradient of a scalar function f can be obtained by noting that $\nabla f = \nabla \cdot (fI)$, where I is the second-order identity tensor

$$\overline{\nabla f(\mathbf{x})} = \nabla \overline{f(\mathbf{x})} + \overline{f \mathbf{n}^S} - \chi \overline{f \bar{\mathbf{n}}}. \quad (2.7)$$

3. Filtered equations of motion

Now the basic LES equations are derived using the above relations. The filtered continuity equation can be obtained by setting $\mathbf{F} = \mathbf{u}$ in Eq.(2.6) and using the continuity equation for the unfiltered velocity. It is

$$\nabla \cdot \bar{\mathbf{u}} = \chi \bar{u}_{\bar{n}}, \quad (3.1)$$

if the velocity on the original boundary is zero.

Using Eqs.(2.6) and (2.7), the momentum equations may be filtered as

$$\begin{aligned} \frac{\partial \bar{\mathbf{u}}}{\partial t} + \nabla \cdot (\mathbf{u} \mathbf{u}) &= -\frac{1}{\rho} \overline{\nabla p} + \nu \overline{\nabla \cdot \nabla \mathbf{u}}, \\ \frac{\partial \bar{\mathbf{u}}}{\partial t} + \nabla \cdot (\mathbf{u} \mathbf{u}) - \chi \overline{\mathbf{u} u_{\bar{n}}} &= -\frac{1}{\rho} (\nabla \bar{p} + \overline{p \mathbf{n}^S} - \chi \bar{p} \bar{\mathbf{n}}) + \nu \left(\nabla \cdot \nabla \mathbf{u} + \frac{\overline{\partial \mathbf{u}}}{\partial n} - \chi \frac{\partial \bar{\mathbf{u}}}{\partial \bar{n}} \right) \end{aligned} \quad (3.2)$$

Noting that $\overline{\nabla \mathbf{u}} = \nabla \bar{\mathbf{u}} - \chi \bar{\mathbf{u}} \bar{\mathbf{n}}$ and $\nabla \cdot \overline{\nabla \mathbf{u}} = \nabla^2 \bar{\mathbf{u}} - \nabla \cdot (\chi \bar{\mathbf{u}} \bar{\mathbf{n}})$, the above equation can be written as

$$\begin{aligned} \frac{\partial \bar{\mathbf{u}}}{\partial t} + \nabla \cdot (\mathbf{u} \mathbf{u}) &= -\frac{1}{\rho} \nabla \bar{p} + \nabla \cdot (\nu \nabla \bar{\mathbf{u}} - \nu \chi \bar{\mathbf{u}} \bar{\mathbf{n}} - \boldsymbol{\tau}) \\ &+ \mathbf{P} + \mathbf{T} + \chi \left(\overline{\mathbf{u} u_{\bar{n}}} - \nu \frac{\partial \bar{\mathbf{u}}}{\partial \bar{n}} \right), \end{aligned} \quad (3.3)$$

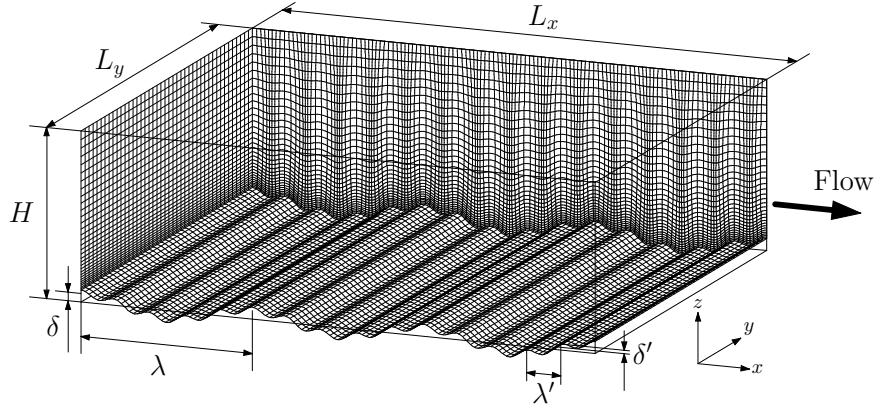


FIGURE 2. DNS of flow over doubly wavy surface.

where

$$\mathbf{P} = \frac{1}{\rho} \overline{p \mathbf{n}}^S = \frac{1}{\rho} \iint_S G(\mathbf{x}, \boldsymbol{\xi}) p(\boldsymbol{\xi}) \mathbf{n} dS_{\boldsymbol{\xi}}, \quad (3.4)$$

$$\mathbf{T} = \nu \overline{\frac{\partial \mathbf{u}}{\partial n}}^S = \nu \iint_S G(\mathbf{x}, \boldsymbol{\xi}) \frac{\partial \mathbf{u}}{\partial n}(\boldsymbol{\xi}) dS_{\boldsymbol{\xi}} \quad (3.5)$$

and $\boldsymbol{\tau}$ is the usual subgrid-scale stress

$$\boldsymbol{\tau} = \rho(\overline{\mathbf{u}\mathbf{u}} - \overline{\mathbf{u}}\overline{\mathbf{u}}). \quad (3.6)$$

We see that in the filtered equations of motion a number of terms appear in addition to the usual subgrid stress. \mathbf{P} and \mathbf{T} are the surface integrals of the pressure and the skin friction over the original surface. Terms associated with χ are quantities that will be important in the near boundary region where χ is nonzero. It should be noted that χ is known once the exact form of the weight function is chosen and the characteristics of the original boundary are given. The terms that need modeling are the surface-average terms \mathbf{P} and \mathbf{T} . These are extra resistances due to the pressure variation and the friction on the smoothed shape of the boundary. Therefore, the direct effects of smoothing the boundary are to introduce extra forces in the momentum equations. The boundary condition of the filtered velocity on the filtered boundary is

$$\overline{\mathbf{u}}(\mathbf{x}_{\overline{S}}) = \iiint_D G(\mathbf{x}_{\overline{S}}, \boldsymbol{\xi}) \mathbf{u}(\boldsymbol{\xi}) d\boldsymbol{\xi}, \quad (3.7)$$

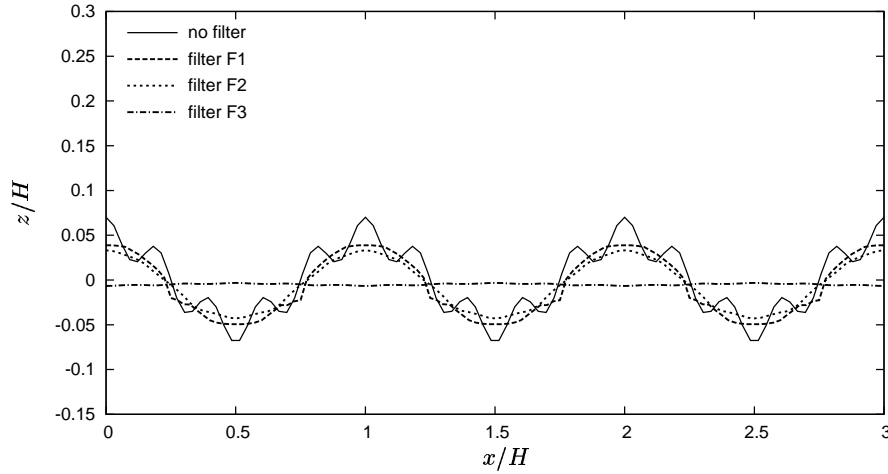
where $\mathbf{x}_{\overline{S}}$ is a point on \overline{S} . We will examine these terms and explore how they may be modeled in the next sections.

4. DNS data of flow over doubly wavy boundary

In order to obtain ideas about how to model the equations derived in the previous section, we have conducted a DNS simulation of a flow over doubly wavy surface, in which the small waviness was intended to simulate roughness and the large waviness the boundary shape (Nakayama & Sakio 2002). Figure. 2 shows the flow field and the

TABLE 1. Size of filters.

Filter	$\Delta_x \times \Delta_y \times \Delta_z$
Filter F1	$\lambda' \times \delta' \times \delta'$
Filter F2	$2\lambda' \times 2\delta' \times 2\delta'$
Filter F3	$2\lambda \times 2\delta \times 2\delta$

FIGURE 3. Smoothed boundary defined by $W_0 = 0.5$.

numerical grid used in this DNS study together with the definition of notation. The details of this simulation are given in Nakayama & Sakio 2002. We explicitly filter the results of this simulation using Eq.(2.1) with different filters. Table 1 shows the sizes of three filters used. They are all top-hat functions for w with Δ_x , Δ_y and Δ_z as the filter width Δ in the x , y , and z directions, respectively. Filter F1 has the same size as the small waviness, F2 is twice as large while F3 is twice as large as the large waviness.

Figure 3 shows the shapes of the smoothed boundary defined by $W_0 = 0.5$. As expected, the shape obtained by filtering with filter F1 removes most of the small waviness, that obtained by filtering with F2 removes the small waviness completely but leaves the large waviness. It is seen that the boundary obtained by filtering with F1 shows a slightly angular shape due to the rectangular top-hat filter used. Filter F3 is large enough to remove all undulations, resulting in an almost flat boundary.

Figure 4 shows the instantaneous flow fields of the DNS results depicted by the surface of constant values of the second invariant of the velocity-gradient tensor. Figure 4(a) is the original unfiltered DNS result while Figure 4(b) is the flow filtered with filter F2. Along with the flow, the boundary is seen to be smoothed and the small structures in the original simulation results are removed. However streaky vortex structures with scales larger than the filter size are still seen. These are what must be reproduced by appropriate LES simulation that does not resolve scales smaller than the the filter size.

The components of \mathbf{P} and \mathbf{T} , tangent to the smoothed boundary, P_s and T_s have been

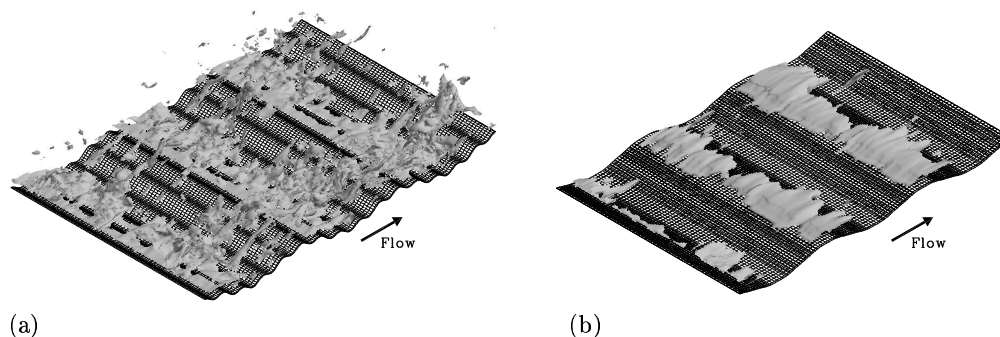


FIGURE 4. Iso-surface of second invariant of velocity gradient tensor in instantaneous DNS results and its filtered flow. (a) unfiltered DNS, (b) filtered DNS.

evaluated using the DNS data and Eqs.(3.4) and (3.5) in order to obtain an idea about these quantities.

Figure 5 shows instantaneous distributions of these terms when filtered with the three filters. It is seen that these terms have significant values in the region near the smoothed boundary. Both terms tend to have positive values where the flow is locally accelerated by the roughness that is smoothed. The pressure integral term P_s tends to have broader distribution and retain large values than the friction integral term as the filter size is increased. The distributions of Figures 5(c) and (f), corresponding to the largest filter size, correspond roughly to the friction and the pressure resistances of the entire waviness.

In addition to the flow over the doubly wavy surface, the flow over a flat surface with small waves has been simulated in order to validate the flow of simpler case of flat rough wall. The small waviness is exactly the same as the small waves of the doubly wavy surface case.

5. Modeling LES equations for rough boundary

Here we consider a method of modeling the LES equations obtained in the previous section. From the analysis it has been seen that it is not just the additive terms in the equations of motion that need modeling but the boundary conditions, and even the position of the boundary, must be modeled. First, as to the position of the boundary, we have already indicated the position where W_0 takes the value $1/2$ for the test flow for which DNS was conducted. The position of the boundary of the computational region and the boundary conditions in LES are related and there may be other choices. We choose the position $W_0 = 0.5$ which corresponds to the real boundary for smooth surface. At this position, however, the filtered velocity is not quite zero and the gradient of W is large but χ is of moderate value. It is not easy to allow leakage through the boundary and nonzero divergence while not violating overall continuity. Here we choose to set the divergence to be zero throughout the analysis region and to require the velocity component normal to the smoothed boundary to vanish. The filtered tangential velocity at the smoothed boundary is roughly the mean velocity in the boundary region. It is closely related to

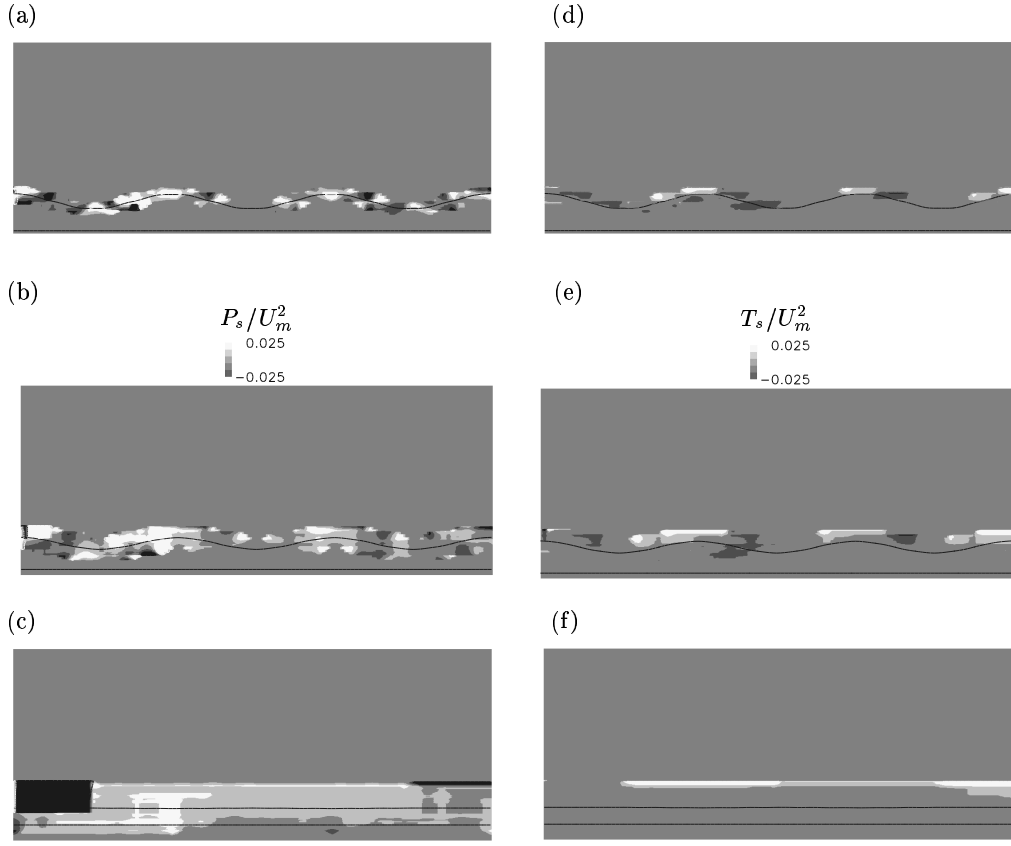


FIGURE 5. Instantaneous distribution of the boundary intergal terms P_s/U_m^2 and T_s/U_m^2 . (a)(d) Filter F1, (b)(e) Filter F2, (c)(f) Filter F3.

the resistance in the same direction. There are a number of resistance formula in various situations including channel flows and even porous flow fields. Generally for flows with high roughness Reynolds numbers, the resistance is proportional to the square of the mean velocity and it is natural to assume a relation like

$$\overline{u_s} = -C_{sl} \text{sign}(R_s) |R_s|^{1/2} \quad (5.1)$$

where R_s is the total resistance $P_s + T_s + \tau_s + \mu \frac{\partial \overline{u_s}}{\partial n}$ at the smoothed boundary, and C_{sl} is a constant. For lower Reynolds numbers, C_{sl} will have to be made a function of the Reynolds number based on the smoothed roughness. Determination of C_{sl} is a critical part of the procedure and it may better be determined dynamically as discussed later.

At this stage it is useful to know what kind of values and distributions that are taken by the quantity χ . They have been calculated for the doubly wavy boundary for the three filters. They are shown in Figure 6. The widths of the distribution are roughly proportional and the magnitudes are inversely proportional to the filter size. The distributions are seen to be more or less linear and this fact may be used in modeling of a rough surface with a given roughness height and filter size.

As to the additional terms in the equations of motion, we propose the following model

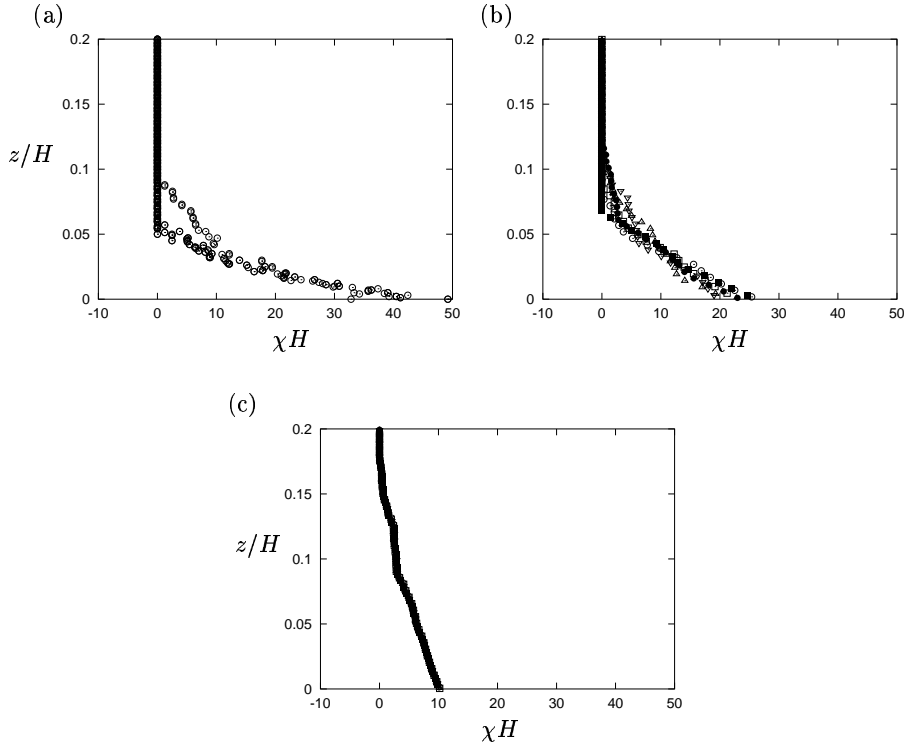


FIGURE 6. Boundary roughness parameter χ . (a) Filter F1, (b) Filter F2, (c) Filter F3, different symbols mean different x locations

for \mathbf{P} and \mathbf{T} .

$$\mathbf{P} = C_d \chi_\Delta \frac{A_\Delta}{\Delta^2} |\mathbf{u}|, \quad (5.2)$$

$$\mathbf{T} = C_f \chi_\Delta \frac{\Sigma_\Delta}{\Delta^2} |\mathbf{u}|, \quad (5.3)$$

where A_Δ and Σ_Δ are the area projected in the direction tangent to the smoothed boundary and the surface area contained in the region proportional to the filter width Δ and C_d and C_f are drag and friction coefficients. We use subscript Δ for χ , A and Σ emphasizing that these depend on the filter size. It should also be noted that the term \mathbf{T} appears even in the case of smooth surface, while \mathbf{P} appears only for rough surfaces. Modeling of \mathbf{T} may then be tested first for simpler smooth surface flow.

6. Test Calculations

Before testing with rough-surface flows, it is useful to see if smooth-surface flow is simulated correctly. The term \mathbf{T} and the boundary conditions are needed for smooth-surface flows and should work as a wall model. It is known that if the laminar sublayer is resolved to a good degree, LES with a Smagorinsky model, either dynamic or standard with appropriate near-wall damping simulates the smooth-wall channel flow. Here a preliminary test calculation has been conducted using two grids with non-slip and slip boundary conditions. The flow is a channel flow with the bulk Reynolds number of 6760.

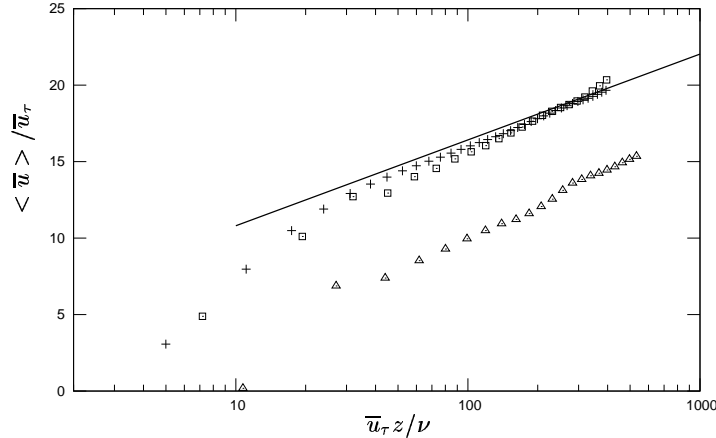


FIGURE 7. The mean velocity profile in smooth-wall channel flow. $-$: standard log-law, $+$: fine grid LES resolving viscous sublayer, \square : coarse grid LES with $C_{sl} = 6$, \triangle : coarse grid LES with $C_{sl} = 0$.

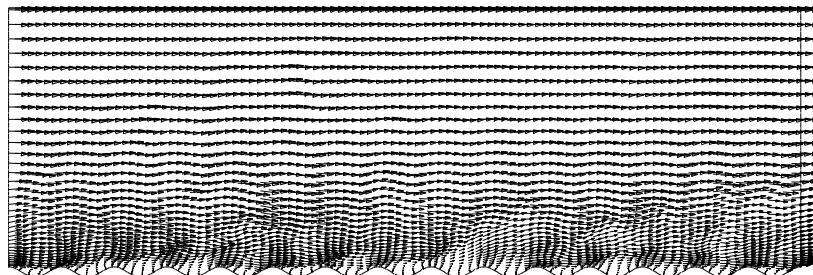
The fine grid has 36 points in the wall-normal direction and the first point near the bottom is about 1.0 viscous length from the wall. The coarse grid has 22 points and the first point is about 10 viscous units away from the boundary. They assume $C_f = 0.002$ and linear distribution for χ with zero filter width.

Figure 7 shows that a LES with fine grid with $C_{sl} = 0$ does reproduce the standard log-law profile. In this smooth-surface case, Σ_Δ/Δ^2 in \mathbf{T} is constant. A coarse-grid LES, however, predicts a mean velocity distribution that is too low. This cannot be improved by adjusting the resistance term \mathbf{T} . The results with $C_{ls} = 6$ is also shown in this figure which indicates the appropriate slip velocity for this Reynolds number. This corresponds to finding the correct off-wall boundary condition and should depend on the Reynolds number and the local flow conditions. Again a dynamic procedure of determining C_{sl} will be more generally applicable.

Next, the flow over flat surface with wavy roughness has been computed. Figure 8(a) shows a snapshot of the velocity field obtained by DNS for this flow. The bulk Reynolds number is again 6760 and the waviness is the same as that of Figure 2. The grid used in LES is $75 \times 36 \times 40$. Figure 8(b) shows the distribution of the time-averaged streamwise velocity component $\langle \bar{u} \rangle$ obtained by LES compared with the DNS results. \bar{u}_τ is the friction velocity defined from the streamwise pressure gradient. The standard smooth-wall log-law is also shown for reference. The boundary drag term now becomes important. In this calculation it is assumed that $C_d = 0.006$ is assumed. It is seen that there is a slight difference in the slope of the logarithmic profile, they agree fairly well, particularly the amount of shift from the smooth line.

Figure 9 now shows the results of the LES calculation of the flow over wavy surface with roughness for which the DNS results have been presented in section 3. The LES grid resolution is such that the small roughness is not resolved but the large waviness is well defined. Figure 9(a) compares the profiles $\langle \bar{u} \rangle$ of the LES with DNS at four locations, at the peak of the waviness, half way to the trough, at the trough and half way to the next peak. Note that the boundary shape used in this calculation is sinusoidal

(a)



(b)

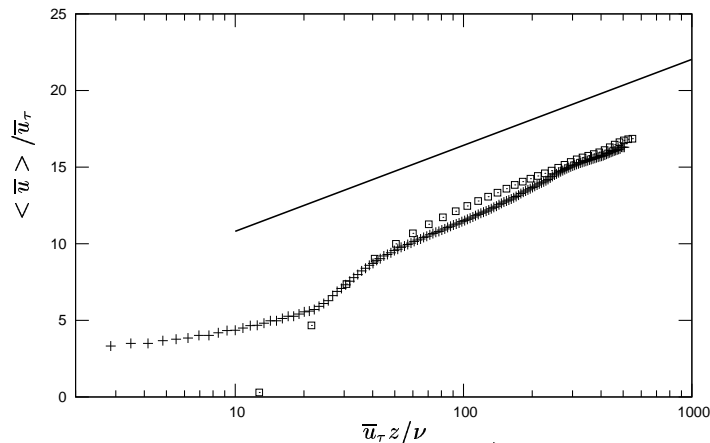


FIGURE 8. Calculation of flow over flat rough surface. (a) Instantaneous velocity distribution from DNS, (b) Mean velocity profile, \square : LES, + : DNS, - : standard smooth log-law.

and z is the distance from the mean boundary position. The values of the constants C_f , C_d and C_{sl} are same as those used for smooth and flat rough surface flows. The profile at the peak is not quite as full as the DNS results and the recirculation region is larger. It implies that the slip velocity is not large enough. The qualitative feature of vortex structure shown in Figure 9(b) seems similar to the filtered DNS flow field shown in Figure 4(b).

7. Dynamic procedure for determining model constants

The test calculations described in the previous section used somewhat ad-hoc values for the model constants. The choice of the values of these constants influences the results very much and they depend on the local and temporal flow conditions. A dynamic method of determining these constants is preferred. Although no detailed calculations are carried out in the present work, a procedure of dynamically determining the model constants has been formulated. The dynamic determination assumes that the same model relation is valid for the filter size implied in the LES calculation and test filtering of larger size. We consider a test filter of size $\tilde{\Delta}$ which is larger than the grid filter size Δ . First it is

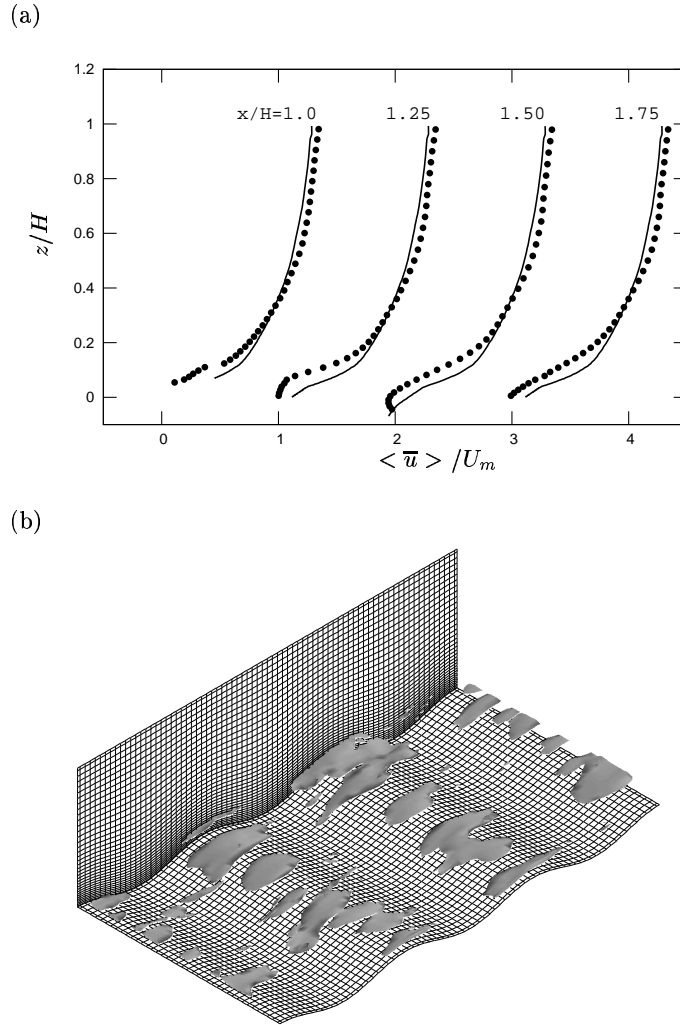


FIGURE 9. Calculation of flow over wavy boundary with roughness. (a) Mean velocity profiles compared with DNS, $-$: DNS, \bullet : LES, profiles for $x/H > 1.0$ shifted horizontally, (b) iso-vorticity surface of LES instantaneous flow results.

noted that test filtering of grid-filtered quantity in finite domain is equal to the single filtering with filter function,

$$G_{\bar{\Delta}}(x, \xi) = \iiint_D G_{\bar{\Delta}}(x, \xi') G_{\bar{\Delta}}(\xi', \xi) d\xi', \quad (7.1)$$

where $\bar{\Delta}$ is the effective filter width of the double filtering. Then we can follow the procedure of Germano *et al.* (1991) and Lilly (1992). The equation for determining constant C_d is as follows.

$$C_d = \frac{\mathbf{R}_p \cdot \mathbf{U}_p}{\mathbf{U}_p \cdot \mathbf{U}_p}, \quad (7.2)$$

where

$$\mathbf{R}_p = \frac{1}{\rho} \bar{p} \tilde{\mathbf{n}}^S, \quad (7.3)$$

is the resistance term resulting from test filtering of size $\bar{\Delta}$ and

$$\mathbf{U}_p = \frac{A_{\bar{\Delta}}}{\bar{\Delta}^2} \chi_{\bar{\Delta}} \left| \tilde{\mathbf{u}} \tilde{\mathbf{u}} \right| - \frac{A_{\Delta}}{\Delta^2} \chi_{\Delta} \left| \mathbf{u} \mathbf{u} \right|, \quad (7.4)$$

Similar equations can be written for constants C_f . Formulation for C_{sl} is a bit different but a similar derivation is possible.

8. Conclusions

Formal explicit filtering defined by the convolution integral over a flow region has been applied to derive fundamental equations of Large Eddy Simulation (LES) for turbulent flows over complex boundaries with small-scale roughness that cannot be resolved. Formal filtering in finite and complex domain allows filtering of the flow and boundary at the same time and indicates that extra stress-like terms appear in the equations. In addition, the boundary condition is no longer nonslip and the boundary velocity must also be modeled. DNS data obtained in a flow over doubly wavy boundary are analyzed to examine the distributions of these terms and to help model these terms. Preliminary LES calculations have been conducted for flow over flat rough surface and the flow over wavy rough surface. It is suggested that the rough boundary effects may be modeled rationally by combination of the boundary resistance and the slip velocity. Although the presently obtained results are with pre-assigned values of the model constants, dynamic procedure to determine model constants has been formulated and its implementation is hoped to make model more general.

REFERENCES

- BROWN, A.R., HOBSON, J.M. & WOOD, N. 2001 Large-eddy simulation of neutral turbulent flow over rough sinusoidal ridges. *Boundary-Layer Meteorology* **98**, 411-441.
- CHOW, F.K. & STREET, R.L. 2002 Modeling unresolved motions in LES of field-scale flows *15th symp. on Boundary Layers and Turbulence*, American Meteorological Society, 432-435, Wageningen, The Netherlands.
- GERMANO, M., PIOMMELLI, U., MOIN, P. & CABOT, W. 1991 A dynamic subgrid-scale eddy viscosity model. *Phys. Fluids* **A3**, 1760-1765.
- LILLY, D.K. 1992 A proposed modification of the Germano subgrid-scale closure method. *Phys. Fluids* **A4**, 633-635.
- NAKAYAMA, A. & SAKIO, K. 2002 Simulation of Flows Over Wavy Rough Boundaries *Center for Turbulence Research, Annual Research Briefs 2002, Stanford University/NASA Ames Research Center*, pp.313-324
- NIKORA, V., GORING, D., MCEWAN, I. & GRIFFITHS, G. 2001 Spatially averaged open-channel flow over rough bed. *J. Hydr. Engrg, ASCE* **127**, 123-133.